

Efficient Minimization of the Non-local Potts Model*

Manuel Werlberger, Markus Unger, Thomas Pock, and Horst Bischof

Institute for Computer Graphics and Vision, Graz University of Technology, Austria
{werlberger, unger, pock, bischof}@icg.tugraz.at
<http://www.icg.tugraz.at>

Abstract. The Potts model is a well established approach to solve different multi-label problems. The classical Potts prior penalizes the total interface length to obtain regular boundaries. Although the Potts prior works well for many problems, it does not preserve fine details of the boundaries. In recent years, non-local regularizers have been proposed to improve different variational models. The basic idea is to consider pixel interactions within a larger neighborhood. This can for example be used to incorporate low-level segmentation into the regularizer which leads to improved boundaries. In this work we study such an extension for the multi-label Potts model. Due to the increased model complexity, the main challenge is the development of an efficient minimization algorithm. We show that an accelerated first-order algorithm of Nesterov is well suited for this problem, due to its low memory requirements and its potential for massive parallelism. Our algorithm allows us to minimize the non-local Potts model with several hundred labels within a few minutes. This makes the non-local Potts model applicable for computer vision problems with many labels, such as multi-label image segmentation and stereo.

1 Introduction

The multiphase partitioning problem consists in finding a certain label for every pixel, tiling the image domain into multiple pairwise disjoint regions. Starting with the seminal work of Mumford and Shah [21] research on computing minimal partitions was ignited by typical Computer Vision problems such as segmentation, stereo or 3D reconstruction. In a discrete version, the Potts model [26], has been known much longer. It was originally invented to model phenomena in solid state mechanics in 1952 and generalizes the two-state model of Ising [18] (1925). The Potts model is a special case of the general multi-labeling problem, relying on a pairwise interaction term that does not assume any ordering of the labels. Minimizing the Potts energy is known to be NP-hard and in general cannot be solved exactly in reasonable time. For this reason various approximations have been proposed to convexify the optimization problem and hence to approximate its solution as effectively as possible.

* This work was supported by the BRIDGE project HD-VIP (no. 827544).

For the two label case, Chan and Vese [12] used the level set framework for optimization but do not yield any optimality. Later, Chan *et al.* [11] showed in a continuous setting that optimality for this problem can be achieved by solving this problem on a relaxed convex set. As the optimization task of the Potts model was originally formulated in a discrete setting, graph cut based approaches have often been used to solve such multi-label tasks. Most notable are move making algorithms of Boykov *et al.* [4] approximately minimizing the Potts model by solving a sequence of globally optimal binary segmentation problems. Although such sequential approaches often generate useful solutions, non of them is able to find a global minimizer. Ishikawa [17] showed that an exact solution can be computed in polynomial time for certain cases, namely when the labels are linearly ordered and the pairwise term is a convex function. Recently, it was shown by Pock *et al.* [25] that the same is true in the continuous case. Unfortunately, the constraint of having linearly ordered labels is not fulfilled in the segmentation task.

For solving the Potts model, several convex relaxations were proposed by *e.g.* Zach *et al.* [34], Lellmann *et al.* [19], Bae *et al.* [2] and Pock *et al.* [24], whereas the latter provides the tightest relaxation with respect to the original problem. The Potts formulation in a spatially continuous setting is given as the energy minimization problem

$$\begin{aligned} \min_{E_l} \left\{ \frac{1}{2} \sum_{l=1}^K \text{Per}(E_l; \Omega) + \sum_{l=1}^K \int_{E_l} f_l(x) dx \right\}, \\ \text{s.t. } \bigcup_{l=1}^K E_l = \Omega, \quad E_i \cap E_j = \emptyset \quad \forall i \neq j, \end{aligned} \tag{1}$$

where the first term measures the interface length of the set E_l enforcing smooth label boundaries and the second term is the data term, a point-wise defined weighting function. Minimizing such an energy partitions the image domain $\Omega \subseteq \mathbb{R}^2$ into K pairwise disjoint regions E_l .

Rewriting the Potts model in terms of a convex total variation optimization problem (*cf.* [34,24,27]) yields the minimization task

$$\begin{aligned} \min_u \{E(u)\} = \min_u \left\{ J(u) + \lambda \sum_{l=1}^K \int_{\Omega} u_l(x) f_l(x) dx \right\}, \\ \text{s.t. } u_l(x) \geq 0, \quad \sum_{l=1}^K u_l(x) = 1, \quad \forall x \in \Omega \end{aligned} \tag{2}$$

with the labeling function $u = (u_1, \dots, u_K) : \Omega \rightarrow [0, 1]^K$ and the weighting function $f = (f_1, \dots, f_K) : \Omega \rightarrow \mathbb{R}^K$. The regularizer $J(u)$ can for example be a simple total variation regularization

$$J(u) = \frac{1}{2} \sum_{l=1}^K \int_{\Omega} |\nabla u_l(x)| dx \tag{3}$$

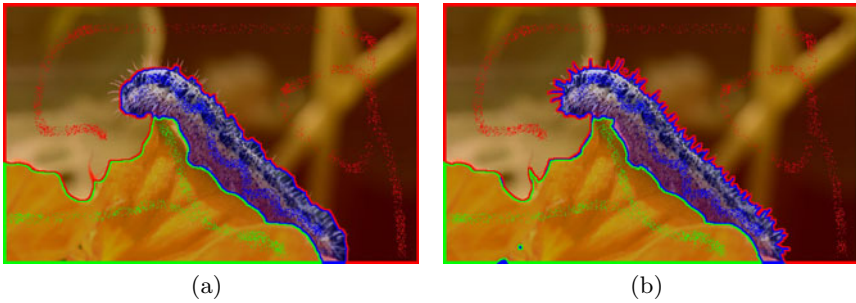


Fig. 1. An example of segmenting an image into 3 different regions. (a) shows the effect on minimizing the interface length and lose fine details like the tiny hairs (although an edge weighing is used) whereas the proposed method (b) is able to preserve those details.

where the minimization results in the perimeter as in (1). As a more sophisticated variant an anisotropic regularization like

$$J(u) = \frac{1}{2} \sum_{l=1}^K \int_{\Omega} \sqrt{\nabla u_l(x)^T D(x) \nabla u_l(x)} dx \quad (4)$$

can be used. $D(x)$ denotes a symmetric tensor for weighting the total variation regularization. A simple variant of this tensor is the weighted total variation $\int_{\Omega} g(x) |\nabla u| dx$, studied by Bresson *et al.* in [7]. It can be obtained by setting

$$D(x) = \text{diag}(g(x), g(x))$$

with an edge detector function $g(x)$, often defined as $g(x) = e^{-\alpha |\nabla I|^\beta}$, with the image gradient ∇I and some $\alpha, \beta > 0$ forcing the total variation regularization towards strong image edges and hence improving the labeling quality. On the other hand, a major drawback is its sensitivity to noise.

In this paper we pursue a different approach to overcome this problem. We include a larger neighborhood in the regularizer $J(u)$ of the multiphase partitioning problem. Adapting the regularization towards local image structures enables the approach to obtain more accurate label boundaries without the dependence on an edge weighting function, which can be very sensitive to noise and strong texture. A result of this approach is depicted in Figure 1. It compares the result of the Potts model incorporating neighborhood relations to the edge-weighted variant on an image of the multi-label benchmark data set [27]. Especially fine structures are preserved and the segmentation results get enhanced towards the users expectations. A related approach was introduced in the field of unsupervised segmentation by Bresson *et al.* [6] where non-local variants of specialized energy functionals are presented by extending the Chan-Vese segmentation [12] and the Mumford-Shah segmentation [21]. While this paper concentrates on the two-label case, we study non-local generalizations of the multi-label Potts

model. The main challenge hereby is the development of an efficient minimization algorithm. To achieve this we adopt the accelerated first-order algorithm of Nesterov [22]. Using this algorithm, we are able to compute the Potts model with several hundred labels.

The contribution of the paper is the definition of the non-local Potts model within a variational framework (Section 2). The efficient minimization using Nesterov's algorithm (Section 3) makes the approach applicable to various Computer Vision Problem. In Section 4 some applications demonstrate the achieved improvements on multi-label segmentation and on disparity estimation of a stereo image pair. The shown examples provide insight into the possibilities of the non-local Potts model and we are convinced that the evident improvements can also be transferred to other Computer Vision problems. Finally, Section 5 concludes our work.

2 Non-local Potts Model

The main intention of the proposed approach is to enhance the labeling quality especially at the label boundaries. Therefore we exploit the affinity of neighboring pixels and steer the regularization towards coherent regions. In terms of image restoration such neighborhood relations have been introduced with *e.g.* the bilateral filtering [29] or non-local means [9], a generalization of the Yaroslavsky filter [32]. For image inpainting, patch-based methods for texture synthesis [14] are related to such non-local approaches and also in stereo applications, Yoon *et al.* [33] incorporated a so-called soft-segmentation to associate certain neighboring pixels for the regularization process. Consequently, the variational interpretation of these neighborhood filters leads to non-local total variation regularization [8,15]. Recently, the approach of non-local regularization in a variational framework was also introduced in the field of optical flow estimation [28,31]. To incorporate neighborhood relations directly into the objective function the non-local total variation regularizer is formulated as

$$J(u) = \sum_{l=1}^K \int_{\Omega} \int_{\mathcal{N}_x} w(x, y) |u_l(y) - u_l(x)| \, dy \, dx \quad , \quad (5)$$

where the function $w(x, y)$ defines the support weights between the pixel x and its neighbors y . The neighborhood system $\mathcal{N}_x \subseteq \Omega$ contains all pixels y with a certain photometric and geometric vicinity around x . The support weight within \mathcal{N}_x is defined in the sense of [33,31] using a low level segmentation combining an Euclidean distance in a color space $\Delta_c(x, y)$ (*e.g.* Lab, RGB or grayscale) and the spatial proximity $\Delta_p(x, y)$ as the Euclidean distance yielding

$$w(x, y) = e^{-\left(\frac{\Delta_c(x, y)}{\alpha} + \frac{\Delta_p(x, y)}{\beta}\right)} \quad . \quad (6)$$

The parameters α and β weight the influence of color similarity and proximity. An exemplary neighboring patch of a specific pixel x is depicted in Figure 2.

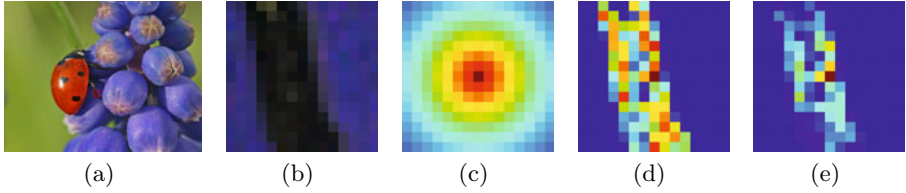


Fig. 2. Exemplar patch (b) of an image (a), the resultant proximity weighting (c), color similarities (d) and the final weighting (e) for the specific neighborhood. x is denoted as a dark red pixel in the center of (c-e), blue color means small weights (reduce regularization influence) and the increasing reddish color shows an increase in the weighting function (strengthen the regularizer).

Using the non-local TV regularizer (5) in the Potts energy (2) yields the energy minimization problem

$$\min_u \left\{ \sum_{l=1}^K \int_{\Omega} \int_{\mathcal{N}_x} w(x, y) |u_l(y) - u_l(x)| \, dy \, dx + \lambda \sum_{l=1}^K \int_{\Omega} u_l(x) f_l(x) \, dx \right\}, \tag{7}$$

$$\text{s.t. } u_l(x) \geq 0, \quad \sum_{l=1}^K u_l(x) = 1 .$$

3 Minimization

Let us first introduce the discrete setting. We consider a Cartesian grid G of size $M_x \times M_y$

$$G = \{(1, 1) \leq (hx, hy) \leq (M_x, M_y)\} ,$$

with the pixel size h and (x, y) the discrete pixel location on the grid. For the ease of presentation we will enumerate the discrete pixel locations (x, y) with an index i , for example by scanning the image domain line by line. The discretized labeling function u is defined on the unit simplex

$$U = \left\{ u = (u_1, \dots, u_K) \in [0, 1]^{K \times M_x \times M_y} : \right. \\ \left. (u_l)_i \geq 0, \quad \sum_{l=1}^K (u_l)_i = 1, \quad i = 1 \dots M_x \times M_y \right\} . \tag{8}$$

The non-negative discrete weighting function for the non-local regularization between discrete pixels i and j is defined as $w_{i,j} \geq 0$. \mathcal{N}_i defines the set of neighbors for pixel i , where $N = |\mathcal{N}_i|$ is the number of pixels within the neighborhood. The weight matrix $(w_{i,j})$ is defined as

$$w_{i,j} = \begin{cases} e^{-\left(\frac{(\Delta_c)_{i,j}}{\alpha} + \frac{(\Delta_p)_{i,j}}{\beta}\right)} & \text{if } j \in \mathcal{N}_i \\ 0 & \text{else} . \end{cases}$$

Now, we are ready to define the non-local gradient operator

$$(\nabla_w u_l)_{i,j} = w_{i,j} ((u_l)_j - (u_l)_i) \text{ ,}$$

which simply holds the weighted non-local pixel differences. Then, (7) can be rewritten in the discrete setting as the following minimization problem

$$\min_u \left\{ \sum_l \|\nabla_w u_l\|_{\ell_1} + \lambda \sum_l \langle u_l, f_l \rangle \right\} \text{ .} \tag{9}$$

Minimizing (9) depicts a convex and non-smooth optimization problem. Solving it with off-the-shelf LP solvers or first-order primal-dual approaches [10] has the problem that each non-local link will demand for a dual variable. For a 512×512 image, 32 labels and a neighborhood size of 15×15 pixels this results in at least one billion dual variables. Hence, these approaches are not feasible for our purposes.

Instead we rely on an old first-order algorithm proposed by Nesterov [22] in 1983, which can be used to minimize a differentiable convex function of a convex set. Furthermore, Nesterov’s algorithm comes along with an improved convergence rate. It can be shown that Nesterov’s algorithm can approach the optimal function value with rate $O(1/n^2)$, where n is the number of iterations. This rate of convergence is still sublinear but improves the convergence rate of standard projected gradient schemes by one order of magnitude. Recently, there are several improved variants using Nesterov’s algorithmic framework [3,30,1,13] and Nesterov himself proposed new algorithms [23]. The major benefit of Nesterov’s first-order primal method is that the algorithm only depends on function values and gradient evaluations which removes the need of the large amount of dual variables. In order to apply Nesterov’s algorithm for our problem (9) we have to find a differentiable approximation of the ℓ_1 norm. We do this by replacing any $|\cdot|$ function by Huber’s function [16].

$$|q|_\varepsilon = \begin{cases} \frac{|q|^2}{2\varepsilon} & |q| \leq \varepsilon \\ |q| - \frac{\varepsilon}{2} & \text{else .} \end{cases}$$

The function is quadratic for small values of ε and linear for the others.

Algorithm: Nesterov’s algorithm for the non-local Potts model: We choose $u^0 = 0, \bar{u}^0 = 0, t^0 = 1$ and iterate for $n \geq 0$.

$$\begin{cases} u_l^{n+\frac{1}{2}} &= \bar{u}_l^n - \frac{1}{L} \left(\nabla_w^T \frac{\nabla_w \bar{u}_l^n}{\max\{\varepsilon, |\nabla_w \bar{u}_l^n|\}} + f_l \right) \text{ , } l = 1, \dots, K \\ u^{n+1} &= \prod_U \left(u^{n+\frac{1}{2}} \right) \\ t^{n+1} &= \frac{1}{2} \left(1 + \sqrt{1 + 4(t^n)^2} \right) \\ \bar{u}_l^{n+1} &= u_l^{n+1} + \frac{t^n - 1}{t^{n+1}} (u_l^{n+1} - u_l^n) \text{ , } l = 1, \dots, K \end{cases} \tag{10}$$

Here, $L = \|\nabla_w\|$ is the norm of the non-local operator which we compute as $L = \frac{4N}{\varepsilon}$ and t^n a variable over-relaxation parameter. The projection \prod_U is an

orthogonal projection onto the unit simplex U . It is known that this projection is highly separable and it can be performed in a finite number of iterations. An exemplary method for computing such successive projections is given in [20].

Although Nesterov's algorithm allows to precompute the maximum number of iterations which are necessary to find an approximate solution in terms of the function values, we found it to be more practical to stop the iterations after the maximal change between two successive iterations is below some threshold. In Figure 3 we compare the convergence of the algorithm for different smoothing parameters ε for an unsupervised segmentation problem. Increasing the smoothing behavior of the Huber function improves the rate of convergence but worsens the approximation quality of the ℓ_1 norm which introduces inaccurate label boundaries. For all our experiments we set $\varepsilon = 0.01$. Observe that after 300 iterations the minimum energy is already attained. For this setup the algorithm runs with 120 iterations/second for an image with size $M_x \times M_y = 404 \times 320$, with $K = 10$ number of labels and a neighborhood size of 7×7 pixels.

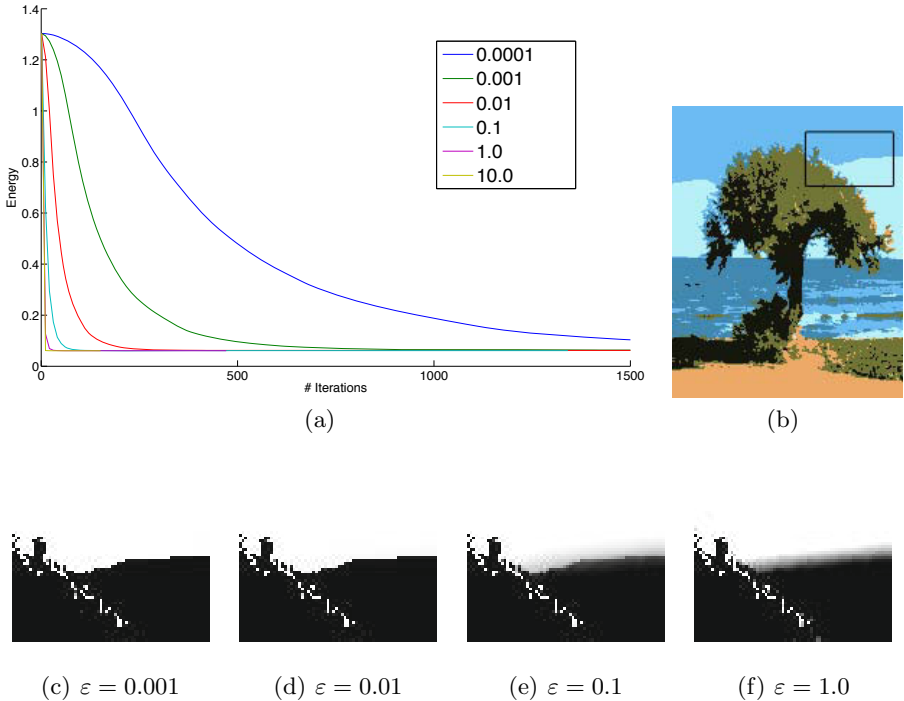


Fig. 3. Comparing convergence behavior of different smoothing parameters ε . (b) is the color-coded labeling result for $\varepsilon = 0.01$ with the marked crop region for (c)-(f) showing a single label u_i for varying ε demonstrating the smoothing effect on label borders for increasing smoothing factors.

4 Applications

4.1 Multi-label Segmentation

Image segmentation is one of the fundamental Computer Vision problems and therefore a vast amount of literature investigates this task. For a general overview on object segmentation we refer to [5]. Very recent work of Santner *et al.* [27] demonstrates the usage of (2) for interactive multi-label segmentation. There, the data term is modeled with different types of features. For a comparison of three different regularization terms, namely the total variation, the edge-weighted and the proposed non-local regularization, we compute a color histogram of scribbles drawn by the user and use this as a feature for the data term in the sense of [27].



Fig. 4. Comparing different regularization terms in terms of interactive multi-label segmentation (*cf.* [27]): TV regularization (first column), edge-weighted TV regularization (second column) and the proposed non-local variant (third column). The scribbles are the users input to mark the corresponding region.

In the first row of Figure 4 the improvement on fine details are visible over all three variants. The edge-weighted TV already yields reasonable accuracy when it comes to segmentation boundaries and with the non-local variant the borders are accurately segmenting the desired region including all fine details. The example in the second row of Figure 4 demonstrates the drawbacks on solely using edges to steer the regularization strength. Sometimes edges that do not coincide with label borders pull the label boundaries away from the desired objects. In Figure 7 we demonstrate especially the improvements on fine details, elongated regions and cavities between labels on segmentation results of the benchmark data set [27].

Next, we want to show the effects when the edge-weighting function of (4) is modified to obtain accurate label boundaries. In Figure 5 an unsupervised labeling routine splits the image domain into several piecewise constant regions.

The data term is solely based on RGB values that are clustered with a standard mean-shift algorithm. Tuning the edge-detector function towards accurate boundaries also introduces some clutter within label regions as a direct consequence of having strong edges within those areas. This weights the regularizer to obtain more and smaller labels and therefore introduces clutter. Using the proposed non-local regularization yields the same precise label borders but also gains a smoother result and keeps coherent regions together.

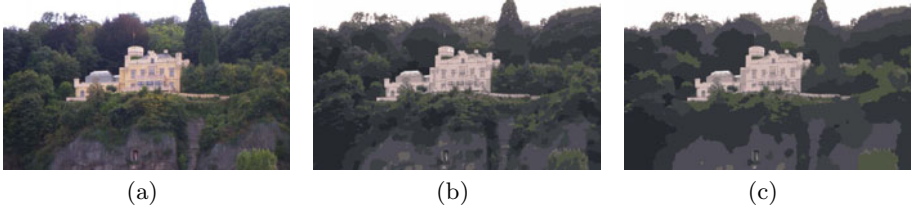


Fig. 5. Unsupervised segmentation splitting an input image (a) into $K = 10$ piecewise constant regions. The tuned edge-weighted regularization (b) achieves nice boundaries but exhibits more clutter within regions compared to the non-local regularization (c).

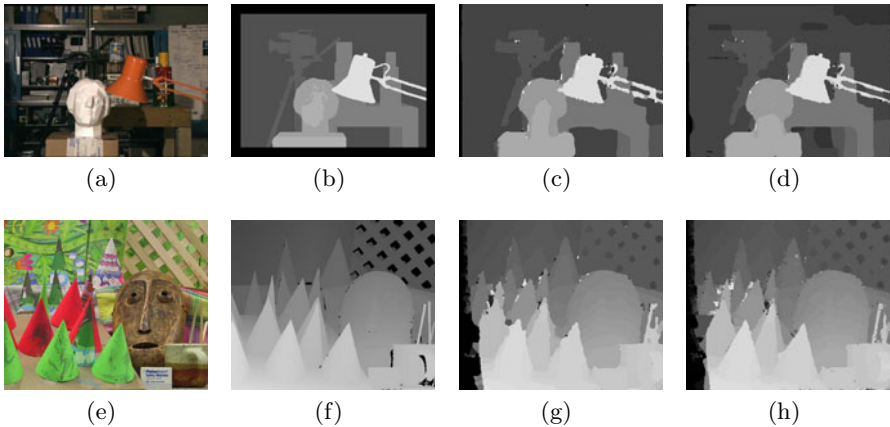


Fig. 6. Disparity estimation of an input image pair (a,e) from the Middlebury stereo data set (<http://vision.middlebury.edu/stereo/>); (b,f) the ground truth disparities; disparity estimation with the Potts model (c,g) and the non-local Potts model (d,h);

4.2 Stereo

As we have already shown the improvements on the image segmentation problem we want to continue with a second Computer Vision problem. We use the Potts model for stereo estimation. The data term for the disparities are modeled using

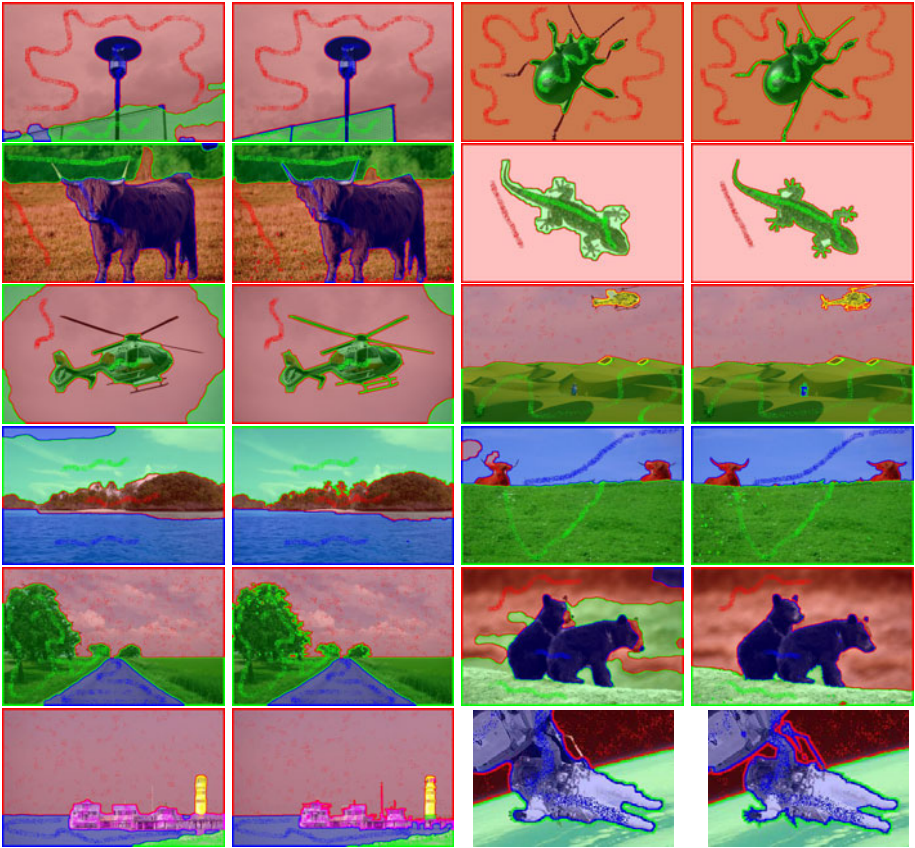


Fig. 7. Multi-Label Segmentation: Comparing results from the edge-weighted Potts model (left image of each pair) and the non-local Potts model (right image of each pair)

absolute differences on gray values. The labels correspond to distinct disparities. For the example in Figure 6 the benefits of the proposed method become apparent with more details and crisper label borders. For the *Tsukuba* image pair (*cf.* first row of Figure 6) the calculation for $M_x \times M_y \times K = 384 \times 288 \times 16$ takes 25 seconds for 500 iterations. For the *Cones* data set (*cf.* second row) with $M_x \times M_y \times K = 450 \times 375 \times 61$ the nonlocal Potts model takes 305 seconds to converge in 1000 iterations. We use a 15×15 neighborhood region for the non-local regularization in both examples.

5 Conclusion

Based on a variational formulation of the Potts model we showed how to incorporate neighborhood relations with a non-local total variation regularization

term. Utilizing low-level image segmentation to steer the regularization towards local image structure enables the method to preserve fine details in the labeling process. The benefits are demonstrating on two typical Computer Vision applications and evident improvements are demonstrated by a comparison with a total variation regularization and its edge-weighted variant. The version of Nesterov's algorithm yields a memory-conscious algorithm and enables the usage of large neighborhoods and several labels with reasonable computational effort.

References

1. Aujo, J.F.: Some first-order algorithms for total variation based image restoration. *J. Math. Imaging Vis.* 34(3), 307–327 (2009)
2. Bae, E., Yuan, J., Tai, X.C.: Global minimization for continuous multiphase partitioning problems using a dual approach. *International Journal of Computer Vision*, 1–18 (2010), doi:10.1007/s11263-010-0406-y
3. Beck, A., Teboulle, M.: A fast iterative shrinkage-thresholding algorithm for linear inverse problems. *SIAM J. Imaging Sci.* 2(1), 183–202 (2009)
4. Boykov, Y., Veksler, O., Zabih, R.: Fast approximate energy minimization via graph cuts. *IEEE Trans. Pattern Analysis and Machine Intelligence* 23(11), 1222–1239 (2001)
5. Boykov, Y.Y., Lea, G.F.: Graph cuts and efficient N-D image segmentation. *International Journal of Computer Vision* 70(2), 109–131 (2006)
6. Bresson, X., Chan, T.F.: Non-local unsupervised variational image segmentation models. Tech. rep., UCLA CAM Report 08-67 (October 2008)
7. Bresson, X., Esedoglu, S., Vandergheynst, P., Thiran, J.P., Osher, S.J.: Fast global minimization of the active contour/snake model. *J. Math. Imaging Vis.* 28(2), 151–167 (2007)
8. Brox, T., Kleinschmidt, O., Cremers, D.: Efficient nonlocal means for denoising of textural patterns. *IEEE Trans. on Image Processing* 17(7), 1083–1092 (2008)
9. Buades, A., Coll, B., Morel, J.M.: Nonlocal image and movie denoising. *International Journal of Computer Vision* 76(2), 123–139 (2007)
10. Chambolle, A., Pock, T.: A first-order primal-dual algorithm for convex problems with applications to imaging. *J. Math. Imaging Vis.* (2010)
11. Chan, T., Esedoglu, S., Nikolova, M.: Algorithms for finding global minimizers of image segmentation and denoising models. *SIAM Journal of Applied Mathematics* 66(5), 1632–1648 (2006)
12. Chan, T., Vese, L.: Active contours without edges. *IEEE Trans. Image Processing* 10(2), 266–277 (2001)
13. Dahl, J., Hansen, P.C., Jensen, S.H., Jensen, T.L.: Algorithms and software for total variation image reconstruction via first-order methods. *Numerical Algorithms* 53(1), 67–92 (2010)
14. Efros, A.A., Leung, T.K.: Texture synthesis by non-parametric sampling. In: *ICCV*, pp. 1033–1038 (1999)
15. Gilboa, G., Osher, S.J.: Nonlocal operators with applications to image processing. Tech. rep., UCLA CAM Report 07-23 (July 2007)
16. Huber, P.J.: *Robust Statistics*. Wiley Series in Probability and Statistics (1981)
17. Ishikawa, H.: Exact optimization for markov random fields with convex priors. *IEEE Trans. Pattern Analysis and Machine Intelligence* 25(10), 1333–1336 (2003)

18. Ising, E.: Beitrag zur Theorie des Ferromagnetismus. *Zeitschrift für Physik* 23, 253–258 (1925)
19. Lellmann, J., Kappes, J., Yuan, J., Becker, F., Schnörr, C.: Convex Multi-class Image Labeling by Simplex-Constrained Total Variation. In: Tai, X.-C., Mørken, K., Lysaker, M., Lie, K.-A. (eds.) *SSVM 2009*. LNCS, vol. 5567, pp. 150–162. Springer, Heidelberg (2009)
20. Michelot, C.: A finite algorithm for finding the projection of a point onto the canonical simplex of \mathbb{R}^n . *Journal of Optimization Theory and Applications* 50, 195–200 (1986)
21. Mumford, D., Shah, J.: Optimal approximation by piecewise smooth functions and associated variational problems. *Comm. Pure Appl. Math.* 42, 577–685 (1989)
22. Nesterov, Y.: A method for solving the convex programming problem with convergence rate $O(1/k^2)$. *Dokl. Akad. Nauk USSR* 269(3), 543–547 (1983)
23. Nesterov, Y.: Smooth minimization of non-smooth functions. *Math. Program.* 103(1, ser. A), 127–152 (2005)
24. Pock, T., Chambolle, A., Cremers, D., Bischof, H.: A convex relaxation approach for computing minimal partitions. In: *IEEE Computer Society Conference on Computer Vision and Pattern Recognition, CVPR* (2009)
25. Pock, T., Cremers, D., Bischof, H., Chambolle, A.: Global solutions of variational models with convex regularization. *SIAM Journal on Imaging Sciences* 3(4), 1122–1145 (2010)
26. Potts, R.B.: Some generalized order-disorder transformations. *Proc. Camb. Phil. Soc.* 48, 106–109 (1952)
27. Santner, J., Pock, T., Bischof, H.: Interactive multi-label segmentation. In: Kimmel, R., Klette, R., Sugimoto, A. (eds.) *ACCV 2010, Part I*. LNCS, vol. 6492, pp. 397–410. Springer, Heidelberg (2011)
28. Sun, D., Roth, S., Black, M.J.: Secrets of optical flow estimation and their principles. In: *IEEE Computer Society Conference on Computer Vision and Pattern Recognition (CVPR)*, San Francisco, CA, USA (June 2010)
29. Tomasi, C., Manduchi, R.: Bilateral filtering for gray and color images. In: *ICCV*, pp. 839–846 (1998)
30. Weiss, P., Blanc-Féraud, L., Aubert, G.: Efficient schemes for total variation minimization under constraints in image processing. *SIAM J. Scientific Computing* 31(3), 2047–2080 (2009)
31. Werlberger, M., Pock, T., Bischof, H.: Motion estimation with non-local total variation regularization. In: *IEEE Computer Society Conference on Computer Vision and Pattern Recognition (CVPR)*, San Francisco, CA, USA (June 2010)
32. Yaroslavsky, L.P.: *Digital Picture Processing — an Introduction*. Springer, Berlin (1985)
33. Yoon, K.J., Kweon, I.S.: Adaptive support-weight approach for correspondence search. *IEEE Trans. on Pattern Analysis and Machine Intelligence* 28(4), 650–656 (2006)
34. Zach, C., Gallup, D., Frahm, J.M., Niethammer, M.: Fast global labeling for real-time stereo using multiple plane sweeps. In: *Proceedings of the Vision, Modeling, and Visualization Conference*, pp. 243–252 (2008)